

Article

An Experimental Study on Ultrasonic Vibration-Assisted Turning of Aluminum Alloy 6061 with Vegetable Oil-Based Nanofluid Minimum Quantity Lubrication

Guoliang Liu ^{1,2,*} , Jin Wang ², Jintao Zheng ², Min Ji ² and Xiangyu Wang ³ 

¹ State Key Laboratory of Mechanical Transmission for Advanced Equipment, Chongqing University, Chongqing 400044, China

² School of Mechanical and Automotive Engineering, Qingdao University of Technology, Qingdao 266520, China; wangjinss1018@163.com (J.W.); zhengjintao_2024@163.com (J.Z.); jimin@qut.edu.cn (M.J.)

³ School of Mechanical Engineering, University of Jinan, Jinan 250022, China; me_wangxy@ujn.edu.cn

* Correspondence: liuguoliang@qut.edu.cn

Abstract: Minimum quantity lubrication (MQL) is a potential technology for reducing the consumption of cutting fluids in machining processes. However, there is a need for further improvement in its lubrication and cooling properties. Nanofluid MQL (NMQL) and ultrasonic vibration-assisted machining are both effective methods of enhancing MQL. To achieve an optimal result, this work presents a new method of combining nanofluid MQL with ultrasonic vibration assistance in a turning process. Comparative experimental studies were conducted for two types of turning processes of aluminum alloy 6061, including conventional turning (CT) and ultrasonic vibration-assisted turning (UVAT). For each turning process, five types of lubricating methods were applied, including dry, MQL, nanofluid MQL with graphene nanosheets (GN-MQL), nanofluid MQL with diamond nanoparticles (DN-MQL), and nanofluid MQL with a diamond/graphene hybrid (GN+DN-MQL). A specific cutting energy and areal surface roughness were adopted to evaluate the machinability. The results show that the new method can further improve the machining performance by reducing the specific cutting energy and areal surface roughness, compared with the NMQL turning process and UVAT process. The diamond nanoparticles are easy to embed on the workpiece surface under the UVAT process, which can increase the specific cutting energy and Sa as compared to the MQL method. The graphene nanosheets can produce the interlayer shear effect and be squeezed into the workpiece, thus reducing the specific cutting energy. The results provide a new way for the development of eco-friendly machining.

Keywords: MQL; nanofluid; ultrasonic vibration-assisted turning; specific cutting energy; areal surface roughness; aluminum alloy 6061



Citation: Liu, G.; Wang, J.; Zheng, J.; Ji, M.; Wang, X. An Experimental Study on Ultrasonic Vibration-Assisted Turning of Aluminum Alloy 6061 with Vegetable Oil-Based Nanofluid Minimum Quantity Lubrication. *Lubricants* **2023**, *11*, 470. <https://doi.org/10.3390/lubricants11110470>

Received: 4 October 2023

Revised: 19 October 2023

Accepted: 31 October 2023

Published: 2 November 2023



Copyright: © 2023 by the authors. Licensee MDPI, Basel, Switzerland. This article is an open access article distributed under the terms and conditions of the Creative Commons Attribution (CC BY) license (<https://creativecommons.org/licenses/by/4.0/>).

1. Introduction

Cutting fluid has been frequently used to improve machinability, including reducing cutting forces and temperature, extending tool life, and improving machined surface integrity, since the early 20th century [1]. However, several drawbacks of the traditional flooded cutting fluids have been confirmed. For example, the cost of cutting fluids accounts for 7–17% of the total manufacturing cost, while its effective availability is relatively low [2,3]. It is difficult to provide the fluid into the cutting area. In addition, most of the cutting fluids used in the processing industry are mineral-based oils, which have huge risk to human health and environmental ecology [4]. Therefore, finding a new reliable machining method with green cutting lubrication technologies has been an extremely urgent task.

In recent years, several sustainable cutting methods have been proposed, including dry cutting, minimum quantity lubrication (MQL), cryogenic cutting, and so on [5–7]. Dry cutting avoids the usage of cutting fluid during the machining process, but often leads to severe tool wear and damaged machined surface integrity because of the bad lubricating and cooling conditions [8]. Cryogenic cutting employs liquid nitrogen, liquid carbon dioxide, or cryogenic gas as the coolant in the process, providing efficient cooling performance without generating pollutants [9]. However, these cryogenic fluids have limited lubricating properties, and their cost is relatively high. In comparison, MQL mixes compressed gas with a tiny amount of cutting fluid to form a droplet mist and generates a high spraying speed, which can obtain a good lubrication effect with a significantly reduced cutting fluid consumption [10]. Furthermore, researchers proved that the adverse effects of mineral-based cutting fluid on the environment and human health can be greatly eliminated by using vegetable oils as the lubricant media [11]. Vegetable oil-based MQL technology has been adopted by many researchers and proved that it can obtain good cutting performance during the machining of different kinds of materials [12].

However, there is a need for further enhancement of the lubrication and cooling properties of the vegetable oil-based MQL droplet mist. The amount of fluid permeating into the cutting zone is minor, although the compressed gas can generate a high spraying speed of droplet mist. According to the existing research, two primary methods are used to enhance the lubrication and cooling properties of MQL. The first involves improving the heat-conducting and lubricating properties of the lubricant media to achieve an effective lubricating and cooling effect with the limited lubricant media. The second approach involves increasing the effective flow rate of droplet mist into the cutting zone to lead to more lubricant media being produced [13,14].

Adding a proper amount of nanoparticles into the vegetable oils to form the nanofluid minimum quantity lubrication (NMQL) process has been proved to be an effective way for further improving the heat-conducting and lubricating properties of the MQL droplets [15]. Researchers have extensively studied the cutting performance of the NMQL process with various kinds of nanoparticles/nanosheets, such as Al_2O_3 , graphite, CNTs, TiO_2 , MoS_2 , hBN, Ag, ZnO, Fe_2O_3 , SiO_2 , and diamond, in different machining methods, including turning, milling, drilling, and grinding [15–20]. It is found that these nanoparticles/nanosheets have different lubricating and cooling properties based on their shape and structural characteristics. The Al_2O_3 and diamond nanoparticles can reduce the tool-chip/workpiece friction coefficient by transforming the sliding friction into rolling friction [15,16]. MoS_2 and graphite have a layered structure with outstanding deposition and film formation properties, which can reduce the friction coefficient by transforming the two sliding metal surfaces to relative slippage of molecular layers [19]. Moreover, the graphite possesses exceptionally high thermal conductivity, ensuring excellent cooling performance during the machining processes [20]. In order to obtain better lubricating and cooling properties, hybrid nanofluid with two or more types of nanoparticles was also designed and tested by some researchers. Sharma et al. [21] performed NMQL turning of AISI 304 steel with Al_2O_3 and graphite as the hybrid nanofluid, and excellent results were observed by considering surface roughness, cutting force, cutting temperature, and tool wear. Jamil et al. [22] combined Al_2O_3 and CNT to form a hybrid nanofluid, and then added cryogenic media to enhance the cooling effect, during the machining of TC4 titanium alloy. A good machining performance was observed.

However, cutting tools are in close contact with the workpieces and chips during the conventional continuous cutting processes. Thus, the nanofluids are blocked from entering the tool-chip/tool-workpiece interfaces, making the lubricating and cooling effect unsatisfying, which is a restriction that has to be urgently settled for NMQL machining processes. In recent years, ultrasonic vibration-assisted machining (UVAM) has been a widely and successfully applied technology in the field of turning, grinding, milling, and drilling [23,24]. The high-frequency vibration of cutting tools can transform the continuous cutting process to an intermittent machining process, thus reducing the cutting force,

cutting temperature, tool wear, and improving the machined surface integrity. In addition, the interrupted cutting action of ultrasonic vibration can break the close contact between the cutting tool and the workpiece/chip, and produce a pumping phenomenon, which can greatly increase the effective flow rate of the cutting fluid. Therefore, combining UVAM with NMQL may produce satisfactory results. Some researchers have attempted to combining different UVAM technologies with the NMQL method. Hoang et al. [25] combined graphene NMQL with an ultrasonic vibration-assisted deep hole drilling process (UVAD) for AISI SUS 304 stainless steel, and found a higher production rate, longer tool life, and better machining performance in terms of cutting forces and processing ability. Gao et al. [26,27] used different types of hybrid nanofluids as an MQL lubricant in ultrasonic vibration-assisted grinding (UVAG) processes. They all proved that the combination of NMQL and UVAG can further decrease the temperature, grinding forces, and friction coefficient.

The above literature review shows the obvious processing advantages of simultaneously using UVAG/UVAD and NMQL methods; however, the experimental confirmation of processing advantages of combining UVAT and NMQL techniques is missing. Thus, this paper aims to investigate the machining performance of UVAT and NMQL methods on aluminum alloy 6061 to experimentally confirm the feasibility of this new machining method. The experimental tests were conducted for different cooling techniques, including dry, MQL using palm oil, and NMQL using diamond nanoparticles, graphene nanosheets, and a hybrid of diamond/graphene mixed in palm oil. Two modes of turning processes, including conventional turning (CT) and ultrasonic vibration-assisted turning (UVAT), were combined with the above cooling techniques. The machining performance of various methods was fully evaluated and compared in terms of their specific cutting energy and areal surface roughness.

2. Experimental Setup and Scheme

The experimental study design aligns with the scheme presented in Figure 1. All cutting experiments are carried out on a CAK3665 CNC lathe (Shenyang Machine Tool Co., Ltd., Shenyang, Liaoning, China) with a self-developed ultrasonic vibration excitation system, as shown in Figure 2a. The Kennametal CCMT 060204 carbide insert (Kennametal, USA) with a tool nose radius of 0.4 mm is used in this work. After being mounted on the ultrasonic horn, the rake angle γ_0 , clearance angle α_0 , and side cutting edge angle K_r of the tool are 0° , 7° , and 5° , respectively, as shown in Figure 2b. Aluminum alloy 6061 is used as the workpiece, and its mechanical properties are shown in Table 1, which were tested by our co-author in a previous study [28]. The radial turning mode is adopted in this work, and ten experiments designed by the single factor experimental design method are shown in Table 2. The cutting speed is selected to guarantee the separation between the tool and chip, while the feed rate and depth of each cut are selected according to the recommendations within the tool manual. During the UVAT processes, an ultrasonic elliptic vibration is applied on the tool nose, and the ultrasonic amplitude in cutting speed direction and depth of cut direction are 3 and 1 μm , respectively. The ultrasonic frequency is 40.8 kHz and the phase difference is 90° . For both MQL and NMQL conditions, the KS-2106 MQL system from Jinzhao Energy Saving Technology Co., Ltd. (Shanghai, China) is adopted. The flow rate for the lubricant is 60 mL/h with a gas pressure of 0.7 MPa. For the NMQL condition, the mass fraction of nanofluids is 0.5%, and the mass ratio of diamond nanoparticles and graphene nanosheets in GN+DN-MQL is 1:1. The size of graphene nanosheets is about 1–3 μm in length and 1–5 nm in thickness. The diameter of diamond nanoparticles is 50 nm. The nanofluid was prepared by dispersing the nanoparticles/nanosheets in palm oil via a two-step method with the Span-80 as the dispersant (mass fraction of 20% of the nanoparticles/nanosheets), i.e., adding a certain amount of nanoparticles/nanosheets and dispersant to base oils followed by sonification (40 kHz, 100 W) for 1 h. According to previous works, the nanoparticles/nanosheets can be dispersed evenly in the palm oil after sonification [29,30].

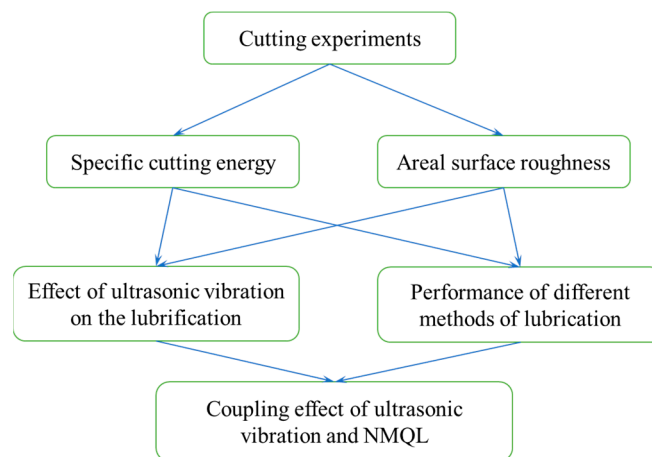


Figure 1. Flow chart of the experimental study.

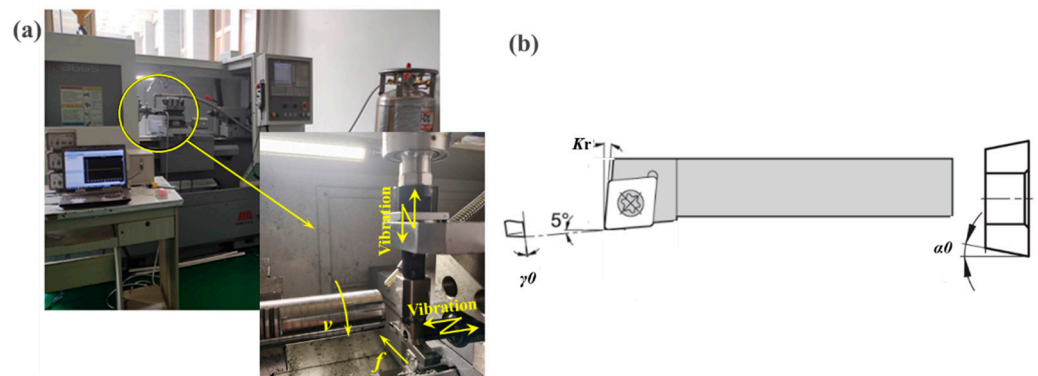


Figure 2. (a) Experimental equipment of the UVAT and NMQL method and (b) the cutting tool angles.

Table 1. The mechanical properties of AA 6061 [28].

Density (g/cm ³)	Tensile Strength (MPa)	Elongation (%)	Hardness (Hv _{9,8} /MPa)
2.75	255	8.17	107.3

Table 2. Cutting test parameters.

Cutting Method	Lubrication Condition	Cutting Speed v (m/min)	Feed Rate f (mm/rev)	Depth of Cut a_p (mm)
CT	Dry	20	0.1	0.1
	MQL			
	GN-MQL			
	DN-MQL			
UVAT	GN+DN-MQL			
	Dry			
	MQL			
	GN-MQL			
	DN-MQL			
	GN+DN-MQL			

CT: conventional turning; UVAT: ultrasonic vibration-assisted turning; MQL: minimum quantity lubrication with palm oil as lubricant; GN-MQL: MQL using graphene nanosheets mixed in palm oil; DN-MQL: MQL using diamond nanoparticles mixed in palm oil; GN+DN-MQL: MQL using diamond/graphene hybrid mixed in palm oil.

During the cutting process, the cutting force in the cutting velocity direction for each cutting condition is measured with a YDC-III89B piezoelectric dynamometer (Dalian University of Technology, Dalian, Liaoning, China), and the specific cutting energy is then calculated. After the turning process, the KEYENCE VK-X1000 laser microscope

(Tokyo, Japan) is used to observe the surface morphology, and then used to measure the areal surface roughness S_a and S_z . The scanning electron microscope (SEM) and energy dispersive spectrometer (EDS) (ZEISS, Tokyo, Japan) are also used to analyze the machined surface morphology and components. A new insert is used in each cutting process to eliminate the errors induced by tool wear and the mounting error, and three tests are conducted for each machining condition to minimize the experimental error.

3. Results and Discussion

3.1. Specific Cutting Energy

Specific cutting energy refers to the energy consumed for removing per unit volume of a workpiece material [31]. The expression for this is $e_s = F_v / (a_p \times f)$, where e_s is the specific cutting energy, F_v is the cutting force in tangential force, a_p is the depth of cut, and f is the feed rate. A lower specific energy indicates an improved lubrication condition [32]. The specific cutting energy of different cutting conditions is shown in Figure 3, and the error bars show the standard deviation of the results among three repetitions. It can be seen from Figure 3 that the ultrasonic vibration reduces the specific cutting energy for all lubrication conditions. It is well-acknowledged that UVAT can reduce the cutting forces by achieving separation between the cutting tool and the chip/workpiece, and thus reduces the specific cutting energy.

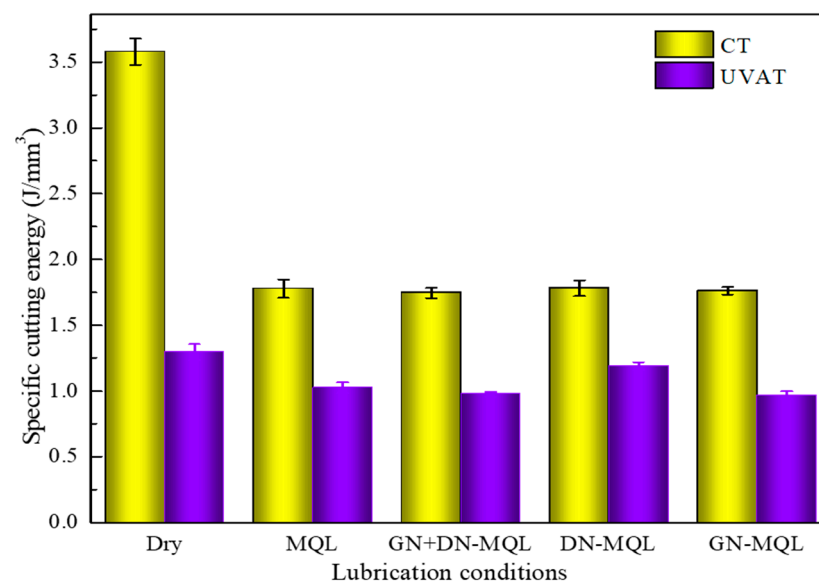


Figure 3. Specific cutting energy of different cutting conditions.

It can also be noticed that, during the CT process, the MQL and NMQL methods with different lubricants all generate significantly lower specific cutting energy in comparison to dry cutting. However, there is no obvious difference between the different MQL and NMQL methods. During the CT process, the cutting tool is in close contact with the workpiece and chip during the whole cutting process, and only a small amount of lubricant can permeate into the cutting zone. In this work, the mass fraction of nanoparticles or nanosheets in nanofluids is very low (only 0.5%). In this case, the nanoparticles or nanosheets that can permeate into the tool/chip or tool/workpiece interfaces to exert a lubrication effect are negligible. Thus, the MQL and NMQL methods fail to produce significant differences among each other regarding specific cutting energy. Certainly, the small quantity of lubricant permeating into the cutting zone can still produce remarkable differences in comparison to dry cutting conditions.

On the contrary, during the UVAT process, not only all the MQL and NMQL methods with different lubricants generate lower specific cutting energy than dry cutting, but the NMQL methods with graphene nanosheets, including GN-MQL and GN+DN-MQL, also

generate lower specific cutting energy than the MQL method which uses pure palm oil. This means that adding graphene nanosheets into the palm oil can further increase the lubrication effect. This was also confirmed by Jia et al. during their investigation of UVAG processes [33]. The results in Figure 3 also prove that the diamond nanoparticles mixed in palm oil have a negative effect on the lubrication effect. This occurs because the DN-MQL method increases the specific cutting energy more in comparison to the MQL method which uses pure palm oil. The ultrasonic vibration can separate the cutting tool and chip/workpiece, and can thus permeate more of the lubricant into the cutting zone. Therefore, the nanoparticles or nanosheets that permeate into the tool/chip or tool/workpiece interfaces can exert a more obvious lubrication effect, resulting in affecting the specific cutting energy differently, as shown in Figure 3.

As for the different effects of graphene nanosheets and diamond nanoparticles on the specific cutting energy, their effects can be attributed to their different shapes and lubrication mechanisms. It has been proved by molecular dynamics simulations, in our previous work, that the tribological behavior of the nano-diamond is dominated by rolling, while the behavior of graphene nanosheets is governed by the interlayer shear effect [34]. During the UVAT processes, the cutting tool constantly bombards the workpiece surface, which can push the nano-diamond and graphene nanosheets into the workpiece. Furthermore, the workpiece material in this work (aluminum alloy 6061) exhibits a low hardness and high plasticity. Therefore, the near-spherical nano-diamond is easy to be squeezed into the workpiece. Once this happens, the nano-diamond will be tightly wrapped by the high-plastic aluminum alloy, and the rolling bearing effect will be severely weakened. Moreover, the nano-diamonds that are embedded on the workpiece surface can work as hard spots and interact with the cutting tool to increase the friction coefficient. This phenomenon is confirmed by the experimental surface morphology shown in Figure 4. It must be noted that the workpiece is cleaned ultrasonically before being observed. Hence, it is reasonably to believe that the large bulge is embedded on the workpiece surface. The results of elemental analysis (Figure 4) also show that the bulge is a mixture of numerous nano-diamonds and aluminum alloy.

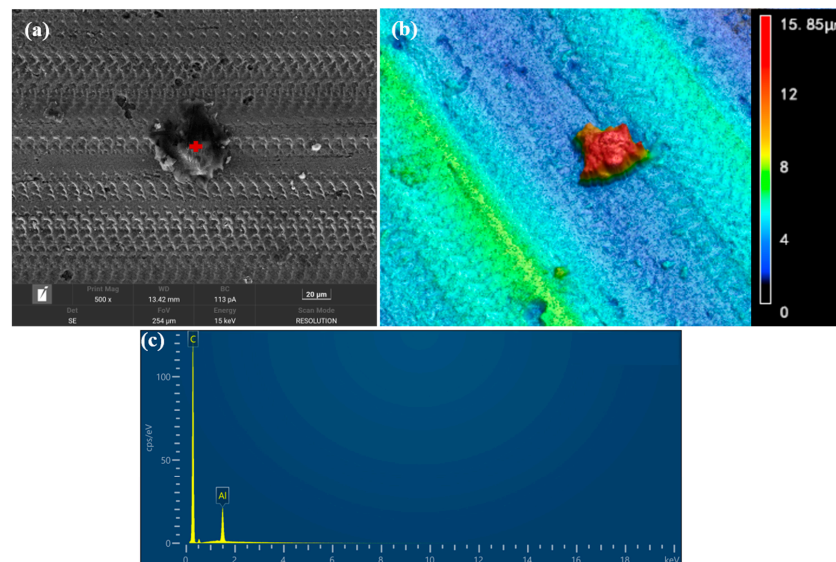


Figure 4. (a) SEM and (b) 3D images ($\times 1000$) of the surface morphology of the UVAT and DN-MQL method, and (c) EDS results of the bulge.

While for the graphene nanosheets, the interlayer shear effect occurs inside the graphene nanosheets. In addition, the graphene nanosheets are relatively large, soft, and more likely to attach to the workpiece and cutting tool surfaces [35]. In this condition, the interlayer shear effect can still work to reduce the cutting forces, even if the graphene

nanosheets are squeezed into the workpiece. Figure 5 shows the experimental surface morphology of the UVAT and GN-MQL method. It can be seen that the graphene nanosheets are squeezed into the workpiece and attached onto the surface. However, the 3D images show that there is no definite upward bulge around the graphene nanosheets. In this case, shear sliding occupies the main position and reduces the friction coefficient.

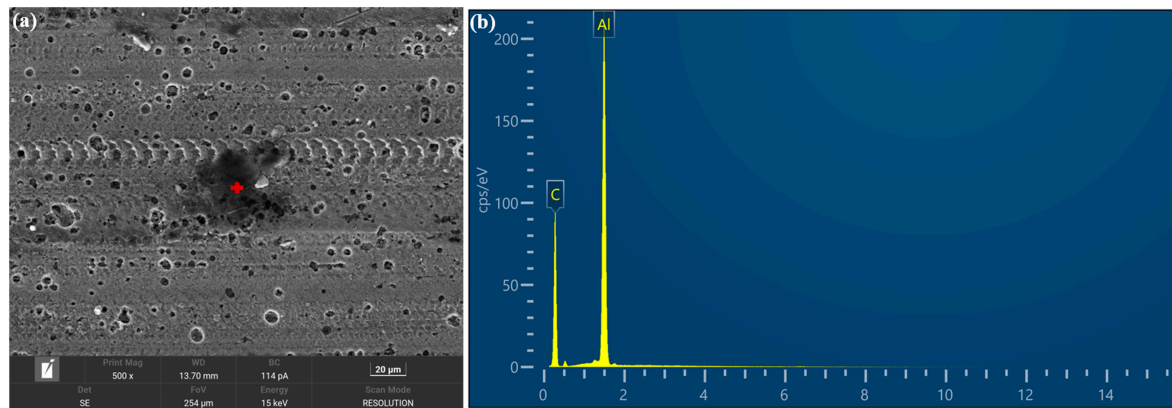


Figure 5. (a) SEM and (b) EDS images of the surface morphology of the UVAT and GN-MQL method.

3.2. Areal Surface Roughness

Figure 6 shows the measured areal surface roughness results under different cutting conditions, and the error bars show the standard deviation of measurement results among three repetitions. S_a is the arithmetic average surface roughness and S_z is the maximum peak-to-valley height of the whole measuring area. It can be seen from Figure 6a that the ultrasonic vibration increases the surface roughness during the dry cutting processes, but generates smoother surfaces under MQL and NMQL conditions. In addition, the lubrication methods show different effects on surface roughness S_a under CT and UVAT processes. During the CT process, MQL with palm oil produces a better surface finish quality than the dry cutting condition, and all the NMQL methods further reduce the surface roughness compared to the MQL condition. While in the UVAT process, the NMQL method with nano-diamond, i.e., DN-MQL, generates a rougher surface in comparison to the MQL condition with palm oil.

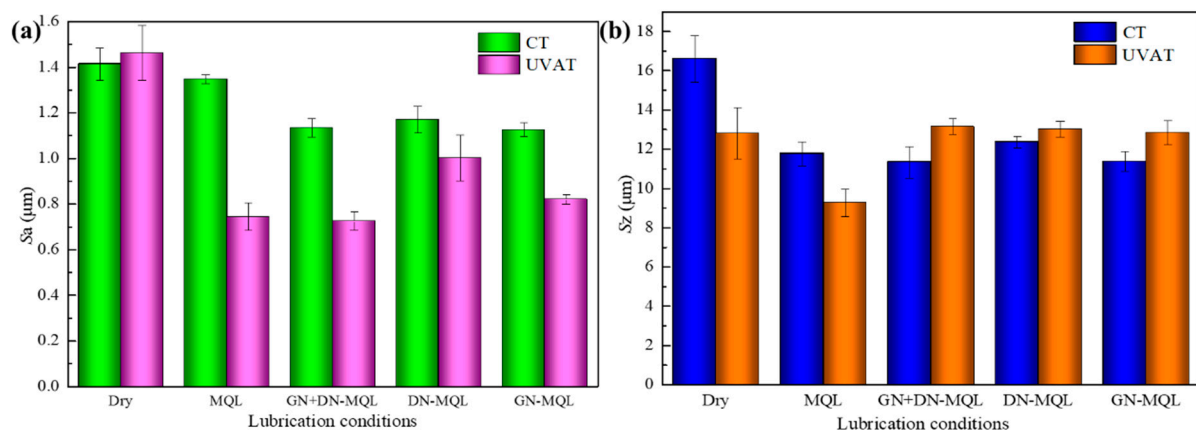


Figure 6. Areal surface roughness, (a) S_a and (b) S_z , of different cutting conditions.

However, when comparing the results of S_z in Figure 6b, the conclusion is different than the one from above. The ultrasonic vibration reduces S_z during dry and MQL conditions in comparison to the CT processes, but generates larger S_z during all NMQL conditions. Among all different lubrication methods, the MQL condition generates the

lowest S_z during both the CT and UVAT processes, and the NMQL methods all reduce S_z in comparison to the dry cutting condition.

Figure 7 shows the surface morphology of the CT and UVAT processes under dry cutting conditions. It can be seen that the ultrasonic vibration generates regular dimples on the machined surface because of the intermittent separation of the cutting tool and workpiece, which increases the average roughness value S_a . However, the ultrasonic vibration amplitude is minor, i.e., $1\ \mu\text{m}$ in the depth of cut direction, and thus the depth of the dimples is very small. Therefore, its effect on surface roughness is minor; thus, the increase rate of S_a is small. On the contrary, the ultrasonic vibration weakened the adhesion between the cutting tool and chip/workpiece, thus reducing the chippings adhered on the machined surfaces. This was also observed by researchers during the UVAG processes [24]. Figure 7a and the EDS results show that the chippings adhered on the machined surfaces are mainly workpiece materials, which are formed by the chips that were squeezed into the surface. Therefore, the S_z value of the UVAT process is lower than that of the CT process.

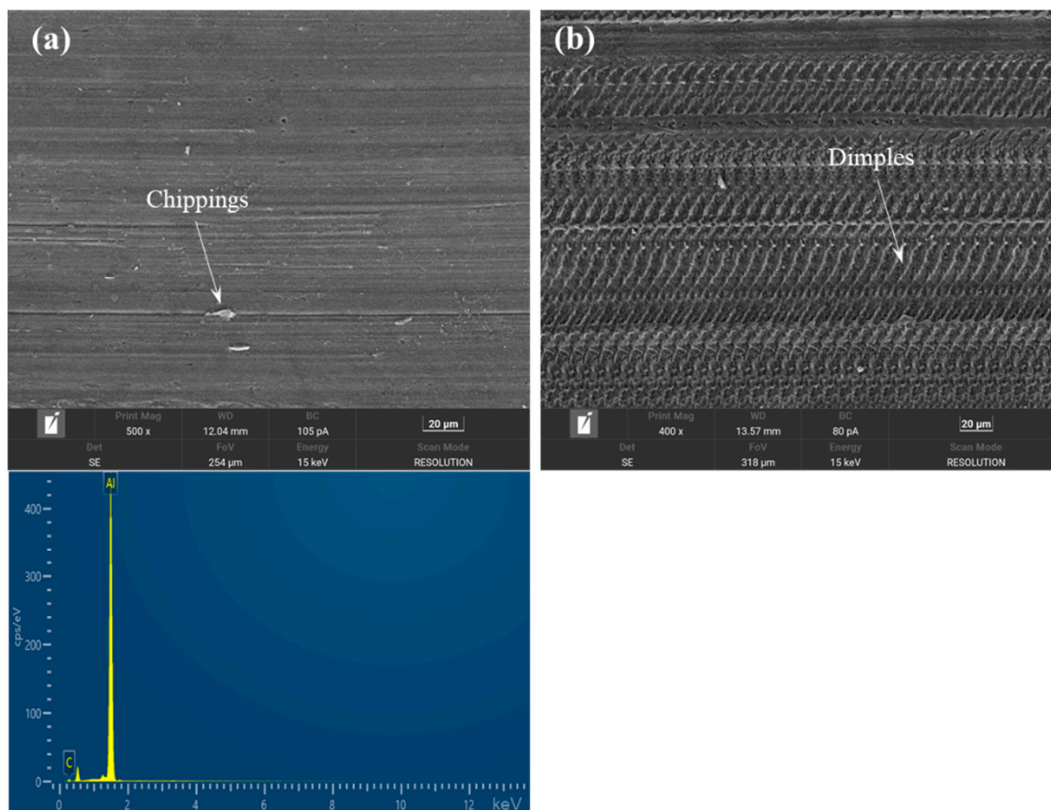


Figure 7. SEM images of the surface morphology of (a) CT and (b) UVAT processes under dry cutting conditions and the EDS results of the chipping in (a).

During the MQL cutting condition, the lubrication effect of palm oil drops can be significantly reinforced via ultrasonic vibration. This can occur as the ultrasonic vibration leads more palm oil drops into the cutting zone. The better lubrication condition can reduce the tool-chip/workpiece adhesion and the side flow of workpiece materials, thus reducing the scallop height between tool paths. This phenomenon can be proved by the 3D images of the surface morphology (Figure 8), and is consistent with the results of Ni et al. [23]. It can be seen from the 3D image, in Figure 8a, that there are obvious plowing marks on the surfaces of the CT process, and the depths of valleys are significantly different. The profile curve fluctuates in a large range from $-6.3\ \mu\text{m}$ to $5.7\ \mu\text{m}$. On the contrary, the surface of the UVAT process, in Figure 8b, is much smoother. The good lubrication condition eliminates the obvious plowing marks. The profile curve in Figure 8b fluctuates in a stable range from

$-2.7\ \mu\text{m}$ to $4.2\ \mu\text{m}$. In this case, the surface roughness of the UVAT and MQL process, including the S_a and S_z , is obviously reduced in comparison to the CT and MQL process.

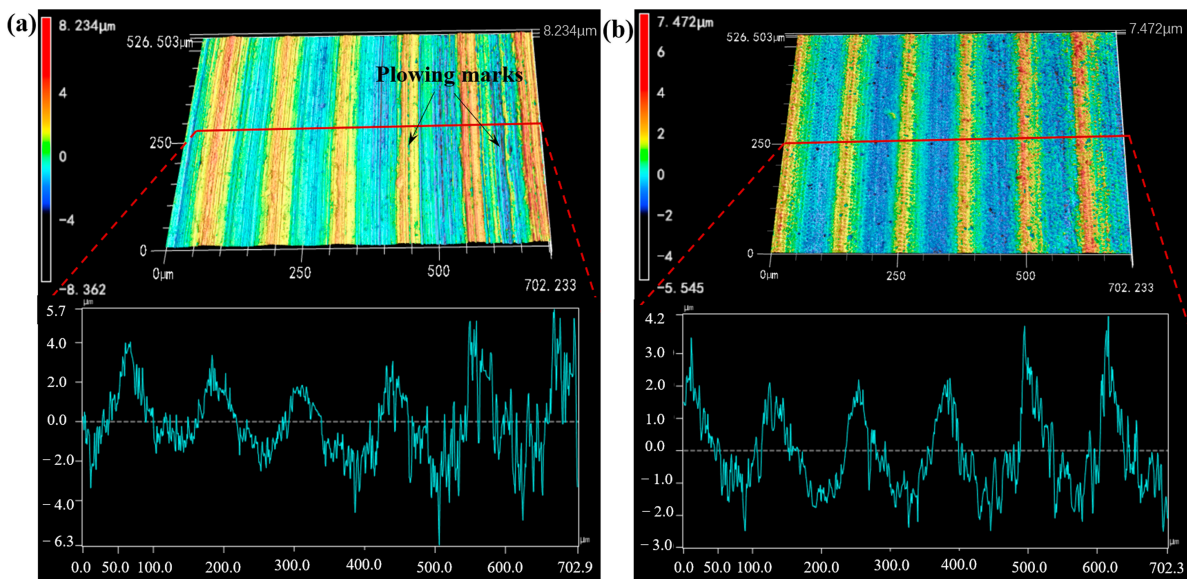


Figure 8. Three-dimensional images ($\times 400$) of the surface morphology of (a) CT and (b) UVAT processes under MQL condition.

When adding nano-diamond or graphene nanosheets into the oil, the lubrication effect of the UVAT and NMQL process can be further improved, thus reducing the average surface roughness S_a in comparison to the CT processes. On the other hand, the nanoparticles/nanosheets can be squeezed into the workpiece using the vibrating cutting tool, thus generating lots of pits after being washed away, as shown in Figure 9. As a result, the S_z value of the UVAT and NMQL process is greater than that of the CT and NMQL process.

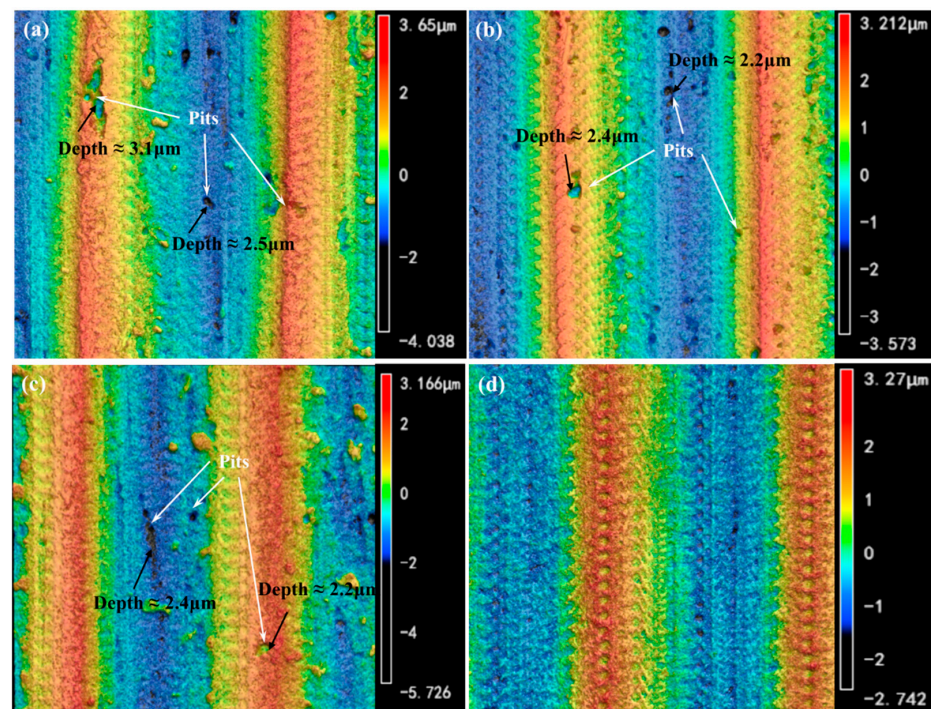


Figure 9. Three-dimensional images ($\times 1000$) of the surface morphology of UVAT processes under (a) DN-MQL, (b) GN-MQL, (c) GN+DN-MQL, and (d) MQL conditions.

In addition, the larger value of S_z in the UVAT and NMQL process than the UVAT and MQL process can also be attributed to the pits generated with the embedded nanoparticles/nanosheets. It is obvious that the surface of the UVAT and MQL process (as shown in Figure 9d) is uniform, and the microstructure produced with ultrasonic vibration is regular, without obvious random defects. On the contrary, the pits resulting from the embedded nanoparticles/nanosheets can be observed on all surfaces of the UVAT and NMQL process. Furthermore, a comparison of the depth of pits in Figure 9 reveals that the UVAT and GN-NMQL process generates relatively shallow pits (the largest depth of pits is 2.4 μm) in comparison to the NMQL conditions which use a nano-diamond material (the largest depth of pits is 3.1 μm).

4. Conclusions

(1) Combining nanofluid MQL with ultrasonic vibration assistance in turning processes has great potential in further improving the machinability in comparison to the NMQL turning process and UVAT process, and has the ability to reduce the specific cutting energy and areal surface roughness.

(2) Due to the low hardness of aluminum alloy 6061, the diamond nanoparticles are easy to embed onto the workpiece surface under the UVAT process, which can significantly weaken their rolling bearing effect and increase the specific cutting energy compared to the MQL method which uses pure palm oil.

(3) The graphene nanosheets can produce the interlayer shear effect by being squeezed into the workpiece. Therefore, the NMQL method which uses a mixture of graphene nanosheets and nano-diamond/graphene nanosheets can further reduce the specific cutting energy compared to the MQL method which uses pure palm oil.

(4) The ultrasonic vibration can significantly reinforce the lubrication effect of the MQL and NMQL methods. The superior lubrication condition can reduce the tool-chip/workpiece adhesion, cutting tool plowing, and workpiece material side flow, thus reducing the average areal surface roughness S_a compared to the CT and MQL as well as CT and NMQL processes.

(5) During the UVAT processes, the nanoparticles/nanosheets can be squeezed into the workpiece with the vibrating cutting tool, thus generating lots of pits on the machined surfaces. Therefore, the surface roughness of the UVAT and NMQL process is increased more in comparison to the UVAT and MQL process.

(6) Future research should be performed to reveal the cutting performance of the UVAT and NMQL process for different kinds of workpiece materials, such as materials with high strength (titanium alloy, for example) and high hardness (quenched steel, for example). Furthermore, more kinds of nanoparticles/nanosheets should be used during the UVAT and NMQL process and the optimal mass fraction of the nanoparticles/nanosheets should be tested.

Author Contributions: Project administration and writing—original draft preparation, G.L.; methodology, J.W.; data curation, J.Z.; writing—review and editing, M.J.; resources, X.W. All authors have read and agreed to the published version of the manuscript.

Funding: This work is financially supported by the Open Research Fund of State Key Laboratory of Mechanical Transmission for Advanced Equipment, Chongqing University (SKLMT-MSKFKT-202105), National Natural Science Foundation of China (52375446 and 52005281), and Natural Science Foundation of Shandong Province (ZR2020QE181).

Data Availability Statement: Data will be made available on request.

Conflicts of Interest: The authors declare no conflict of interest.

References

1. Said, Z.; Gupta, M.; Hegab, H.; Arora, N.; Khan, A.M.; Jamil, M.; Bellos, E. A comprehensive review on minimum quantity lubrication (MQL) in machining processes using nano-cutting fluids. *Int. J. Adv. Manuf. Technol.* **2019**, *105*, 2057–2086. [[CrossRef](#)]

2. Amiril, S.A.S.; Rahim, E.A.; Syahrullail, S. A review on ionic liquids as sustainable lubricants in manufacturing and engineering: Recent research, performance, and applications. *J. Clean. Prod.* **2017**, *168*, 1571–1589. [[CrossRef](#)]
3. Yıldırım, Ç.V.; Sarıkaya, M.; Kıvık, T.; Şirin, Ş. The effect of addition of hBN nanoparticles to nanofluid-MQL on tool wear patterns, tool life, roughness and temperature in turning of Ni-based Inconel 625. *Tribol. Int.* **2019**, *134*, 443–456. [[CrossRef](#)]
4. Abd Rahim, E.; Dorairaju, H. Evaluation of mist flow characteristic and performance in minimum quantity lubrication (MQL) machining. *Measurement* **2018**, *123*, 213–225. [[CrossRef](#)]
5. Liu, G.L.; Zheng, J.T.; Huang, C.Z.; Sun, S.F.; Liu, X.F.; Dai, L.J.; Wang, X.Y. Coupling effect of micro-textured tools and cooling conditions on the turning performance of aluminum alloy 6061. *Adv. Manuf.* **2023**, *11*, 663–681. [[CrossRef](#)]
6. Guolong, Z.H.A.O.; Lianjia, X.I.N.; Liang, L.I.; Zhang, Y.; Ning, H.E.; Hansen, H.N. Cutting force model and damage formation mechanism in milling of 70wt% Si/Al composite. *Chin. J. Aeronaut.* **2023**, *36*, 114–128.
7. Liu, K.; Zhang, J.; Li, J.; Bao, R.; Zuo, Y.; Liu, H.; Wang, Y. Experiment study of surface formation mechanism during cryogenic turning of PEEK. *J. Manuf. Process.* **2023**, *104*, 322–333. [[CrossRef](#)]
8. Şirin, Ş.; Sarıkaya, M.; Yıldırım, Ç.V.; Kıvık, T. Machinability performance of nickel alloy X-750 with SiAlON ceramic cutting tool under dry, MQL and hBN mixed nanofluid-MQL. *Tribol. Int.* **2021**, *153*, 106673. [[CrossRef](#)]
9. Albertelli, P.; Strano, M.; Monno, M. Simulation of the effects of cryogenic liquid nitrogen jets in Ti6Al4V milling. *J. Manuf. Process.* **2023**, *85*, 323–344. [[CrossRef](#)]
10. He, T.; Liu, N.; Xia, H.; Wu, L.; Zhang, Y.; Li, D.; Chen, Y. Progress and trend of minimum quantity lubrication (MQL): A comprehensive review. *J. Clean. Prod.* **2022**, *386*, 135809. [[CrossRef](#)]
11. Hybská, H.; Mitterpach, J.; Samešová, D.; Schwarz, M.; Fialová, J.; Veverková, D. Assessment of ecotoxicological properties of oils in water. *Arch. Environ. Prot.* **2018**, *44*, 31–37.
12. Sankaranarayanan, R.; Krolczyk, G.M. A comprehensive review on research developments of vegetable-oil based cutting fluids for sustainable machining challenges. *J. Manuf. Process.* **2021**, *67*, 286–313.
13. Wang, X.; Li, C.; Zhang, Y.; Ding, W.; Yang, M.; Gao, T.; Ali, H.M. Vegetable oil-based nanofluid minimum quantity lubrication turning: Academic review and perspectives. *J. Manuf. Process.* **2020**, *59*, 76–97. [[CrossRef](#)]
14. Kumar, A.; Sharma, A.K.; Katiyar, J.K. State-of-the-art in sustainable machining of different materials using nano minimum quantity lubrication (NMQL). *Lubricants* **2023**, *11*, 64. [[CrossRef](#)]
15. Gupta, M.K.; Jamil, M.; Wang, X.; Song, Q.; Liu, Z.; Mia, M.; Imran, G.S. Performance evaluation of vegetable oil-based nano-cutting fluids in environmentally friendly machining of inconel-800 alloy. *Materials* **2019**, *12*, 2792. [[CrossRef](#)]
16. Yıldırım, Ç.V. Experimental comparison of the performance of nanofluids, cryogenic and hybrid cooling in turning of Inconel 625. *Tribol. Int.* **2019**, *137*, 366–378. [[CrossRef](#)]
17. Darshan, C.; Jain, S.; Dogra, M.; Gupta, M.K.; Mia, M. Machinability improvement in Inconel-718 by enhanced tribological and thermal environment using textured tool. *J. Therm. Anal. Calorim.* **2019**, *138*, 273–285. [[CrossRef](#)]
18. Musavi, S.H.; Davoodi, B.; Niknam, S.A. Effects of reinforced nanoparticles with surfactant on surface quality and chip formation morphology in MQL-turning of superalloys. *J. Manuf. Process.* **2019**, *40*, 128–139. [[CrossRef](#)]
19. Das, A.; Pradhan, O.; Patel, S.K.; Das, S.R.; Biswal, B.B. Performance appraisal of various nanofluids during hard machining of AISI 4340 steel. *J. Manuf. Process.* **2019**, *46*, 248–270. [[CrossRef](#)]
20. Lim, S.K.; Azmi, W.H.; Jamaludin, A.S.; Yusoff, A.R. Characteristics of Hybrid Nanolubricants for MQL Cooling Lubrication Machining Application. *Lubricants* **2022**, *10*, 350. [[CrossRef](#)]
21. Sharma, A.K.; Tiwari, A.K.; Dixit, A.R.; Singh, R.K.; Singh, M. Novel uses of alumina/graphene hybrid nanoparticle additives for improved tribological properties of lubricant in turning operation. *Tribol. Int.* **2018**, *119*, 99–111. [[CrossRef](#)]
22. Jamil, M.; Khan, A.M.; Hegab, H.; Gong, L.; Mia, M.; Gupta, M.K.; He, N. Effects of hybrid Al₂O₃-CNT nanofluids and cryogenic cooling on machining of Ti–6Al–4V. *Int. J. Adv. Manuf. Technol.* **2019**, *102*, 3895–3909. [[CrossRef](#)]
23. Ni, C.; Zhu, L. Investigation on machining characteristics of TC4 alloy by simultaneous application of ultrasonic vibration assisted milling (UVAM) and economical-environmental MQL technology. *J. Mater. Process. Technol.* **2020**, *278*, 116518. [[CrossRef](#)]
24. Kumar, M.N.; Subbu, S.K.; Krishna, P.V.; Venugopal, A. Vibration assisted conventional and advanced machining: A review. *Procedia Eng.* **2014**, *97*, 1577–1586. [[CrossRef](#)]
25. Hoang, T.D.; Ngo, Q.H.; Chu, N.H.; Mai, T.H.; Nguyen, T.; Ho, K.T.; Nguyen, D. Ultrasonic assisted nano-fluid MQL in deep drilling of hard-to-cut materials. *Mater. Manuf. Process.* **2022**, *37*, 712–721. [[CrossRef](#)]
26. Gao, T.; Zhang, X.; Li, C.; Zhang, Y.; Yang, M.; Jia, D.; Zhu, L. Surface morphology evaluation of multi-angle 2D ultrasonic vibration integrated with nanofluid minimum quantity lubrication grinding. *J. Manuf. Process.* **2020**, *51*, 44–61. [[CrossRef](#)]
27. Rabiei, F.; Rahimi, A.R.; Hadad, M.J. Performance improvement of eco-friendly MQL technique by using hybrid nanofluid and ultrasonic-assisted grinding. *Int. J. Adv. Manuf. Technol.* **2017**, *93*, 1001–1015. [[CrossRef](#)]
28. Wang, J.; Duan, P.; Wang, T.; Wang, X.; Qiao, Y. Effect of Cryogenic Cooling on Mechanical Properties and Cutting Force of 6061 Aluminum Alloy. *J. Phys. Conf. Ser.* **2023**, *2459*, 012032. [[CrossRef](#)]
29. Zhang, Y.; Li, C.; Jia, D.; Zhang, D.; Zhang, X. Experimental evaluation of the lubrication performance of MoS₂/CNT nanofluid for minimal quantity lubrication in Ni-based alloy grinding. *Int. J. Adv. Manuf. Technol.* **2015**, *99*, 19–33. [[CrossRef](#)]
30. Su, Y.; Gong, L.; Li, B.; Liu, Z.; Chen, D. Performance evaluation of nanofluid MQL with vegetable-based oil and ester oil as base fluids in turning. *Int. J. Adv. Manuf. Technol.* **2016**, *83*, 2083–2089. [[CrossRef](#)]
31. Shaw, M.C.; Cookson, J.O. *Metal Cutting Principles*; Oxford University Press: New York, NY, USA, 2005.

32. Liu, G.; Özel, T.; Li, J.; Wang, D.; Sun, S. Optimization and fabrication of curvilinear micro-grooved cutting tools for sustainable machining based on finite element modelling of the cutting process. *Int. J. Adv. Manuf. Technol.* **2020**, *110*, 1327–1338. [[CrossRef](#)]
33. Jia, D.; Li, C.; Zhang, Y.; Yang, M.; Zhang, X.; Li, R.; Ji, H. Experimental evaluation of surface topographies of NMQL grinding ZrO₂ ceramics combining multiangle ultrasonic vibration. *Int. J. Adv. Manuf. Technol.* **2019**, *100*, 457–473. [[CrossRef](#)]
34. Wang, D.; Zhang, Y.; Zhao, Q.; Jiang, J.; Liu, G.; Li, C. Tribological mechanism of carbon group nanofluids on grinding interface under minimum quantity lubrication based on molecular dynamic simulation. *Front. Mech. Eng.* **2023**, *18*, 17. [[CrossRef](#)]
35. Hoang, T.D.; Mai, T.H.; Nguyen, V.D. Enhancement of Deep Drilling for Stainless Steels by Nano-Lubricant through Twist Drill Bits. *Lubricants* **2022**, *10*, 173. [[CrossRef](#)]

Disclaimer/Publisher's Note: The statements, opinions and data contained in all publications are solely those of the individual author(s) and contributor(s) and not of MDPI and/or the editor(s). MDPI and/or the editor(s) disclaim responsibility for any injury to people or property resulting from any ideas, methods, instructions or products referred to in the content.